

# Improvement of diffraction efficiency of flat-panel coherent backlight for holographic displays

Wei Hu, Chao Ping Chen, Yan Li, Zhenghong He, Xiao Li, Pengcheng Zhou, Jiangang Lu, and Yikai Su\*

National Engineering Lab for TFT-LCD Materials and Technologies, Department of Electronic Engineering, Shanghai Jiao Tong University, Shanghai 200240, China  
[yikaisu@sjtu.edu.cn](mailto:yikaisu@sjtu.edu.cn)

**Abstract:** Coherent backlight is an essential component for holographic displays. In this paper, a compact design of edge-lit coherent backlight featuring two holographic optical elements for two-dimensional beam expansion is presented. Its diffraction efficiency is numerically studied using the coupled-wave theory. In experiments, the diffraction efficiency is measured as 4.3% and the feasibility of this design is verified by reconstructing 3D images with a spatial light modulator.

©2015 Optical Society of America

**OCIS codes:** (080.1665) Coherent design; (050.7330) Volume gratings; (090.2870) Holographic display; (230.3720) Liquid-crystal devices; (090.2890) Holographic optical elements.

---

## References and links

1. P. A. Blanche, A. Bablumian, R. Voorakaranam, C. Christenson, W. Lin, T. Gu, D. Flores, P. Wang, W. Y. Hsieh, M. Kathaperumal, B. Rachwal, O. Siddiqui, J. Thomas, R. A. Norwood, M. Yamamoto, and N. Peyghambarian, "Holographic three-dimensional telepresence using large-area photorefractive polymer," *Nature* **468**(7320), 80–83 (2010).
2. X. Li, C. P. Chen, H. Gao, Z. He, Y. Xiong, H. Li, W. Hu, Z. Ye, G. He, J. Lu, and Y. Su, "Video-rate holographic display using azo-dye-doped liquid crystal," *J. Disp. Technol.* **10**(6), 438–443 (2014).
3. X. Li, C. P. Chen, Y. Li, X. Jiang, H. Li, W. Hu, G. He, J. Lu, and Y. Su, "Color holographic display based on azo-dye-doped liquid crystal," *Chin. Opt. Lett.* **12**(6), 060003 (2014).
4. T. Kozacki, G. Finke, P. Garbat, W. Zaperty, and M. Kujawińska, "Wide angle holographic display system with spatiotemporal multiplexing," *Opt. Express* **20**(25), 27473–27481 (2012).
5. A. Putilin and I. Gustomiasov, "Application of holographic elements in displays and planar illuminators," *Proc. SPIE* **6637**, 66370N (2007).
6. I. Shariv, Y. Amitai, and A. A. Friesem, "Compact holographic beam expander," *Opt. Lett.* **18**(15), 1268–1270 (1993).
7. W.-C. Su, C.-C. Sun, and N. Kukhtarev, "Multiplexed edge-lit holograms," *Opt. Eng.* **42**(7), 1871–1872 (2003).
8. H. Ueda, E. Shimizu, and T. Kubota, "Image blur of edge-illuminated holograms," *Opt. Eng.* **37**(1), 241–246 (1998).
9. J. Upatnieks, "Edge-illuminated holograms," *Appl. Opt.* **31**(8), 1048–1052 (1992).
10. R. Shechter, Y. Amitai, and A. A. Friesem, "Compact beam expander with linear gratings," *Appl. Opt.* **41**(7), 1236–1240 (2002).
11. Y. Xiong, Z. He, C. P. Chen, X. Li, A. Li, Z. Ye, J. Lu, G. He, and Y. Su, "Coherent backlight system for flat-panel holographic 3D display," *Opt. Commun.* **296**, 41–46 (2013).
12. H. Kogelnik, "Coupled wave theory for thick hologram gratings," *Bell Syst. Tech. J.* **48**(9), 2909–2947 (1969).
13. Z. He, C. P. Chen, H. Gao, Q. Shi, S. Liu, X. Li, Y. Xiong, J. Lu, G. He, and Y. Su, "Dynamics of peristrophic multiplexing in holographic polymer-dispersed liquid crystal," *Liq. Cryst.* **41**(5), 673–684 (2014).
14. S.-T. Wu and D. K. Yang, *Reflective Liquid Crystal Displays* (Wiley, 2001), Chap. 6.
15. M. Born and E. Wolf, *Principles of Optics* (Cambridge university, 1999).
16. J. Qi, L. Li, M. De Sarkar, and G. P. Crawford, "Nonlocal photopolymerization effect in the formation of reflective holographic polymer-dispersed liquid crystals," *J. Appl. Phys.* **96**(5), 2443–2450 (2004).
17. L. Lesem, P. Hirsch, and J. Jordan, "The kinoform: a new wavefront reconstruction device," *IBM J. Res. Develop.* **13**(2), 150–155 (1969).
18. G. McPherson, *Statistics in Scientific Investigation* (Springer, 1990).
19. C. Gu, J.-R. Lien, F. Dai, and J. Hong, "Diffraction properties of volume holographic diffusers," *J. Opt. Soc. Am. A* **13**(8), 1704–1711 (1996).
20. S. Wadle, D. Wuest, J. Cantalupo, and R. S. Lakes, "Holographic diffusers," *Opt. Eng.* **33**(1), 213–218 (1994).
21. V. Toal, *Introduction to Holography* (CRC, 2011).

## 1. Introduction

Holography is considered as an ultimate three-dimensional (3D) technique because it can exactly reconstruct the wavefront and thus render a 3D scene naturally [1–3]. Holography is a technique based on interference, which requires high coherence of light. Thus lasers are the optimum light sources. In current holographic display systems, the laser beams are expanded to a proper size using lenses groups [4]. These optical components are usually too bulky to be applied in consumer electronics, especially for flat-panel display devices. In order to address this issue, a coherent backlight with a compact form factor is necessary to realize flat-panel holographic displays.

Although some efforts have been made on compact expanders for lasers using optical folding method or edge-illuminated holograms [5–9], they can only expand the beam in one dimension. In another compact beam expander introduced by Revital *et al.* [10], the output are discrete multiple light spots which cannot be used as an entire plane wave. In our previous work, Xiong *et al.* [11] proposed a two-dimensional coherent backlight design using a scattered wave to read out a reflection hologram. Nevertheless, its diffraction efficiency (DE) is as low as 0.3%, which is a critical problem to resolve towards practical applications.

In this paper, we analyze the factors limiting the DE of the system proposed in [11] with coupled-wave theory. The low DE in the previous design [11] was mainly caused by the random phase of the scattered wave. Moreover, a coherent backlight design is proposed that can improve the DE to ~4.3%, which is one order in magnitude higher than the previous result [11]. In our design, the first holographic optical element expands beam spot in the vertical direction and the second holographic optical element expands the beam in the horizontal direction. As a result, a two-dimensional expansion is achieved. To verify the feasibility, 3D holographic images are reconstructed using this coherent light.

## 2. Flat-panel coherent backlight design

### 2.1 Theoretical analysis and numerical results

The coherent backlight structure in [11] was based on the principle of holography. In that work, a volume hologram was formed by a scattered wave and a plane wave, and then the scattered wave was used to reconstruct the plane wave. The DE, defined as a ratio of the intensity of the reconstructed plane wave to that of the incident scattered wave, is about 0.3%, which is too low for practical applications.

The analytical solutions of DE using Kogelnik's coupled-wave theory [12] is derived in the Appendix. The numerical result of DE using a scattered wave to reconstruct a plane wave is shown in Fig. 1 (red triangular line). On the other hand, the numerical result of DE using a set of plane-wave components to read out a plane wave is plotted in Fig. 1 (black circular line).

As one can see from Fig. 1, there is a periodical correlation between DE and position  $z$  inside the hologram. The DE is considered in the case that  $z$  is equal to the thickness of the hologram, in both simulation and experiment. The DE for a transmission volume phase grating under Bragg condition can be written as [12]:

$$\eta = \sin^2\left(\frac{\Delta\phi}{2}\right) = \sin^2\left(\frac{\pi n_1 d}{\lambda \cos\theta}\right) \quad (1)$$

where  $\Delta\phi$  is the phase modulation,  $n_1$  is the amplitude of refractive index modulation,  $d$  is the thickness of the hologram, and  $\theta$  is the Bragg angle of the incident light within the material. The simulated hologram is recorded by a plane wave and a scattered wave which can be regarded as the superposition of multiple linear gratings. As the position  $z$  inside the hologram varies, the phase modulation of each grating changes, which leads to a varied DE.

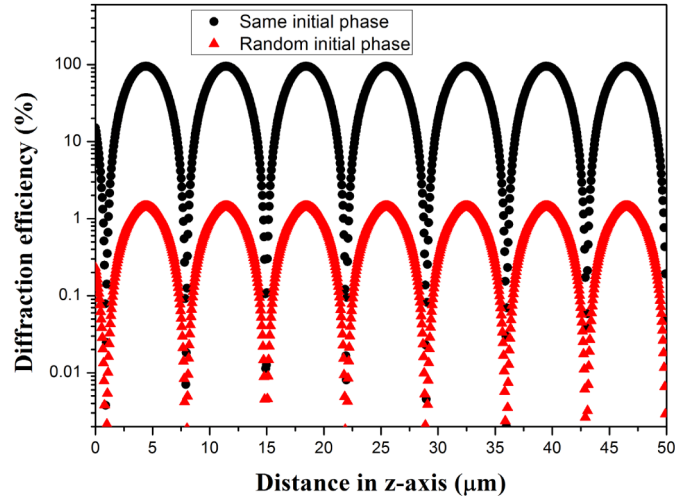


Fig. 1. DE of the hologram [11] versus distance in z-axis. Z-axis is defined in Fig. 9 in Appendix.

The result (red triangular line in Fig. 1) is higher than the experimental result (0.3%) [11] because many other factors are not considered in this model, such as reflections from the interfaces, vibrations of the platform and so on. However, one can still find out that the random phase of the scattered wave results in a significant decrease in DE as in Fig. 1. In the hologram, the refraction index modulation is the superposition of that of multiple gratings. Each grating has a random phase shift which is uniform in probability statistics as each plane-wave component in scattered wave has a random phase. Consequently, the total refraction index modulation is averaged out, resulting in low DE.

### 2.2 Schematic flat-panel backlight setup

To improve the DE, a wave without random phase can be used to replace the scattered wave. We use two holographic optical elements (HOEs) to expand a laser beam in two dimensions to achieve both compact structure and higher DE.

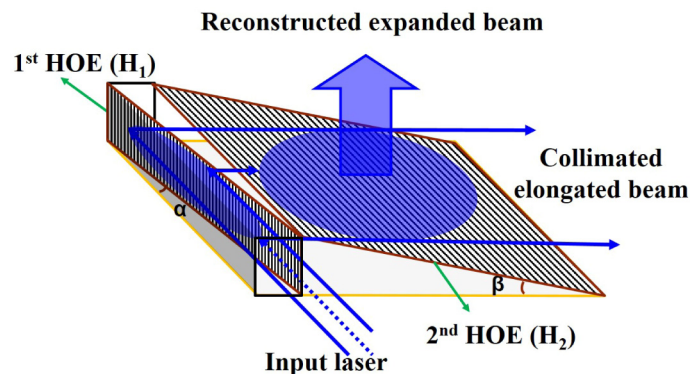


Fig. 2. Schematic drawing of the proposed coherent backlight structure.

The schematic drawing of the proposed flat-panel backlight design is depicted in Fig. 2. It consists of two HOEs, which are essentially two linear gratings. The first HOE  $H_1$  is used to expand a laser beam in the vertical direction as an elongated beam, which is further expanded in the horizontal direction by the second HOE  $H_2$ . Therefore, two-dimensional beam expansion is realized, and the expanded beam is coherent and uniform, which could be used

as the backlight for holographic displays. The slant angles of the HOEs  $\alpha$  and  $\beta$  should be properly set to guarantee a compact form. The propagation direction of undiffracted wave is perpendicular to the diffracted direction to reduce disturbance. All the other higher diffraction orders are negligible since both two HOEs are transmission volume holograms [12]. To avoid Bragg mismatch and to achieve high DE during the process of reading, the reading beam,  $H_1$ , and  $H_2$  should be firmly fixed relative to each other.

It should be noticed that  $H_1$  and  $H_2$  are not equivalent to two mirrors, through which the shape and size of the laser beam keep unchanged upon the mirror reflection. Moreover, the HOEs can diffract light wave to pre-defined directions, while the mirrors can only reflect light wave in the direction that is symmetrical to the incident direction.

### 3. Experiments and results

A proof-of-concept experiment is carried out to prove the feasibility of the proposed backlight. Furthermore, the expanded wave is projected onto a spatial light modulator (SLM) (PLUTO, Holoeye) to display holographic 3D images.

We use two plane waves to record the HOEs as both of them are linear gratings. The material used in the experiment is polymer dispersed liquid crystal (PDLC) [13], which comprises 50 wt%: 35.4 wt%: 13 wt%: 1 wt%: 0.6 wt% of liquid crystal 5CB (HCCH): TMPTA monomer (Aldrich): N-vinylpyrrolidone (Aldrich): N-phenylglycine (Aldrich): Rose Bengal (Aldrich). The uniform PDLC mixture is injected into an empty cell, whose thickness is controlled by 30- $\mu\text{m}$  Mylar spacers.

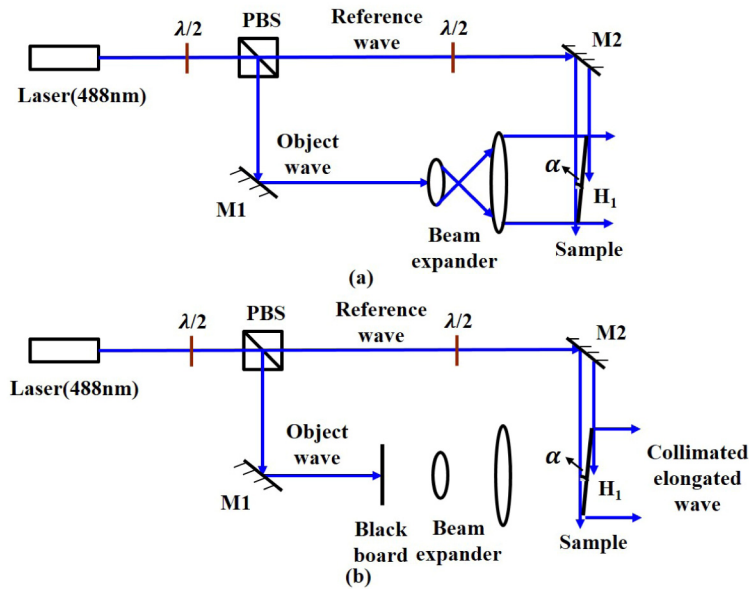


Fig. 3. Experimental setup for  $H_1$  (a) recording and (b) reconstruction. PBS: polarizing beam splitter; M1, M2: mirrors;  $\lambda/2$ : half wave plate.

Figures 3(a) and 3(b) illustrate the experimental setups for  $H_1$  recording and reconstruction, respectively. In Fig. 3(a), light derived from a 488 nm laser is set to s-polarization to ensure high interference efficiency as the recording angle is almost  $90^\circ$ . The reference beam is emitted from the laser with a diameter  $\sim 0.1$  cm and the area of the spot is  $\sim 0.0079$   $\text{cm}^2$ . The slant angle  $\alpha$  of  $H_1$  is  $\sim 6^\circ$  which enables the reference beam to illuminate an elongated elliptic area ( $\sim 0.075$   $\text{cm}^2$ ) on  $H_1$ . In addition, the object beam is expanded to 1 cm in diameter by a conventional beam expander in Fig. 3(a). The intensities of both recording waves are 2  $\text{mW}/\text{cm}^2$  on  $H_1$ , and the exposure time is 1 min. In Fig. 3(b), the object plane

wave is blocked by a black board and the reference beam reconstructs a collimated elongated beam, which further interferes with another plane wave in  $H_2$  recording process.

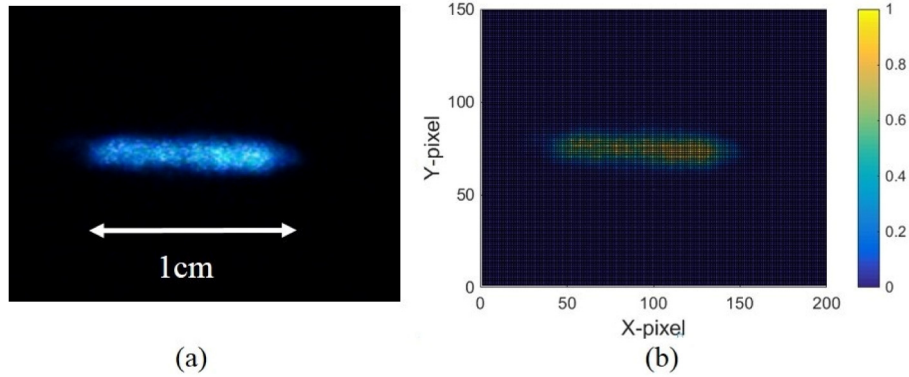


Fig. 4. (a) Image of diffracted waves of  $H_1$ , (b) normalized intensity distribution of the pattern.

As shown in Fig. 4(a), the collimated elongated beam with an area of  $\sim 0.075 \text{ cm}^2$  is reconstructed by the reading beam. The intensity of the collimated elongated beam is almost uniform, as shown in Fig. 4(b). The power of the elongated beam is measured to be 0.033 mW when the power of the reading beam is 0.158 mW. The DE of  $H_1$  is 21%, defined as the ratio of the power of the reconstructed collimated elongated wave to that of the reading beam.

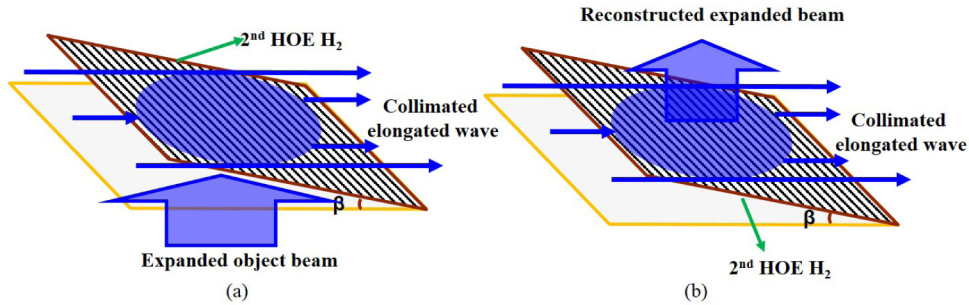


Fig. 5. Schematic drawings of  $H_2$  during (a) recording and (b) reconstruction.

We use the collimated elongated wave generated by  $H_1$  as the reference beam, and a circularly expanded beam from a conventional beam expander as an object beam, to record  $H_2$  as shown in Fig. 5(a). Because the interbeam angle is  $\sim 90^\circ$ , both waves are set to s-polarization to maximize the interference efficiency. The slant angle  $\beta$  of  $H_2$  is  $\sim 6^\circ$ , and the collimated elongated wave illuminates a circular area ( $\sim 0.7 \text{ cm}^2$ ) on  $H_2$ . The object plane wave is expanded to 1 cm in diameter. The intensities of both recording waves are  $1 \text{ mW/cm}^2$ , and the exposure time is 2 mins.

Figure 6(a) shows the reconstructed expanded beam with a power 0.0068 mW when the power of the reading beam is 0.158 mW. Figure 6(b) is the normalized intensity distribution. The definition of the total DE is the ratio of the power exiting  $H_2$  to the incident power on  $H_1$ . The DE is measured to be 4.3%, which is one order of magnitude higher than our previous result in [11]. However, the expanded plane wave is round or elliptical in shape while the shape of SLM is rectangular which implies part of the output wave cannot be used. Both  $H_1$  and  $H_2$  are PDLC cells with sizes of  $2 \text{ cm} \times 2.5 \text{ cm}$ . The size of the proposed compact beam expander is measured to be  $2.5 \text{ cm} \times 2.3 \text{ cm} \times 0.5 \text{ cm}$  in the proof-of-concept experiment. Moreover, for practical applications, the thickness of 0.5 cm could be reduced to 0.1 cm with optimized design, which is orders of magnitude lower than that of the lenses based

conventional beam expander, while the laser beam is expanded to a plane wave with a diameter of 1 cm.

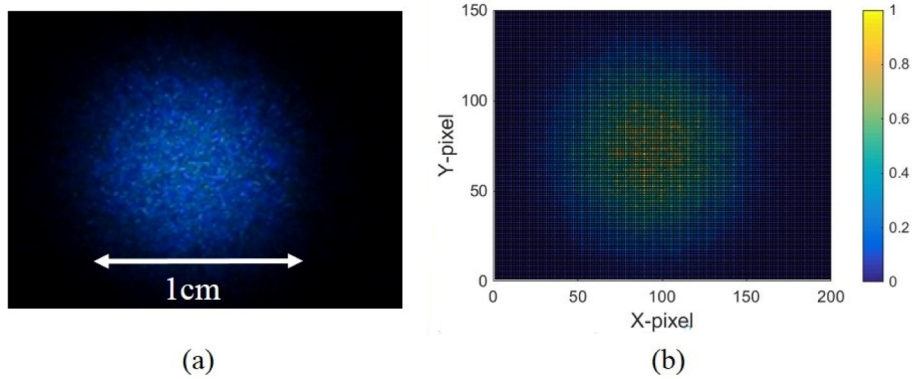


Fig. 6. (a) Image of diffracted waves of  $H_2$ , (b) normalized intensity distribution of the pattern.

Each HOE in our system is a transmission volume hologram. It is known that the DE of a volume hologram can reach  $\sim 90\%$ . However, the DE of each HOE in the experiment is  $\sim 21\%$ , which can be attributed to the following reasons.

Firstly, part of the energy of the reading beam could be absorbed by the residual photoinitiator Rose Bengal (RB) in the PDLC cell in the reconstruction process. Suppose that the scattering can be neglected, the transmittance  $T$  of a PDLC film cured between two glass plates can be estimated as [14]:

$$T = (1 - R)^2 \exp(-\alpha l) \quad (2)$$

where  $R$  is the reflectance at a single air-glass interface,  $l$  is the light path length through the medium,  $\alpha$  is the absorption coefficient. To measure the transmittance, a PDLC cell is exposed under uniform light for 3 minutes. The reflectance  $R$  is estimated to be  $\sim 4\%$  as the refractive index of glass is  $\sim 1.5$  according to Fresnel law [15]. The transmittance is measured to be  $\sim 67\%$  while the reading beam (488 nm, s-polarization) is normal incident on the PDLC cell. In this case, the path length of the beam in the medium is equal to the thickness of the PDLC cell ( $20 \mu\text{m}$ ). Therefore the absorption coefficient can be calculated to be  $\sim 164\text{cm}^{-1}$ . The absorption could be decreased by reducing the ratio of RB in the PDLC cell.

Secondly, the reflection on the interfaces should be considered in the reconstruction processes of HOEs  $H_1$  and  $H_2$ . The reflectance is almost 40% while the incident angle of the reading beam is  $\sim 84^\circ$  when the reading beam illuminates on  $H_1$  or  $H_2$ . This is due to the refractive index mismatch between different layers, and the large incident angle. This issue could be solved through anti-reflection coating or refractive index matching process between multiple layers.

Thirdly, according to the work reported by Qi *et al.* [16], the grating cannot be formed perfectly in PDLCs when the grating pitch is on the order of hundreds of nanometers. In the experiment, the grating pitch of each expander is  $\sim 400 \text{ nm}$ , implying that the formation of the grating could be incomplete.

One can predict that the DE of each HOE could be enhanced to  $\sim 49\%$  in case of lower absorption of the material, and if the anti-reflection issue is properly solved. Therefore the total DE could be improved to  $\sim 24\%$ , higher than the optical efficiencies of conventional liquid crystal displays (LCDs).

The reconstructed expanded beam is projected onto the SLM loaded with a computer generated hologram (CGH) to achieve holographic displays. The CGH based on Kinoform algorithm [17] is also used in the previous work [11]. The reconstructed 3D image consists of

a letter 'A' located at 2 m away from the SLM, and a letter 'B' located at 1 m away from the SLM.

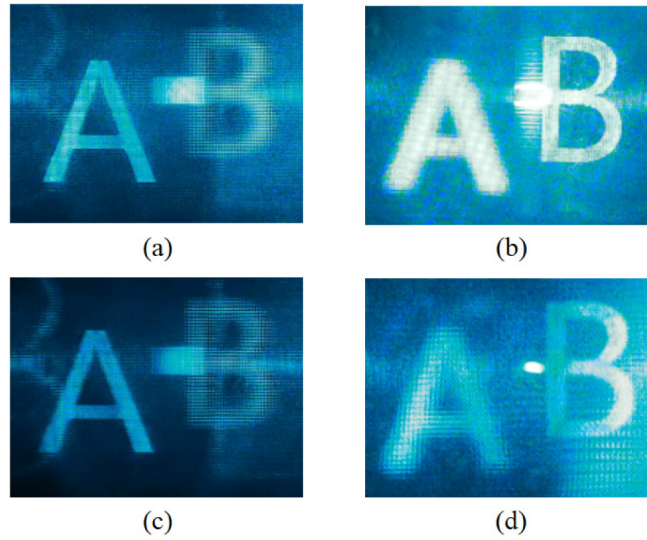


Fig. 7. Holographic 3D images reconstructed with a SLM using a conventional beam expander and focuses on (a) 'A', (b) 'B'; using the proposed compact beam expander and focuses on (c) 'A', (d) 'B'.

As shown in Fig. 7, we use the conventional beam expander and the proposed compact beam expander to generate expanded collimated beams, which are incident onto the SLM to read out the holographic 3D images, respectively. In Figs. 7(a) and 7(b), one can see that when the camera focuses on one letter, that letter is clear in focus, while the other is out of focus, thus becoming blurred. As seen in Figs. 7(c) and 7(d), there is a little distortion in the 3D images formed by the reconstructed expanded beam.

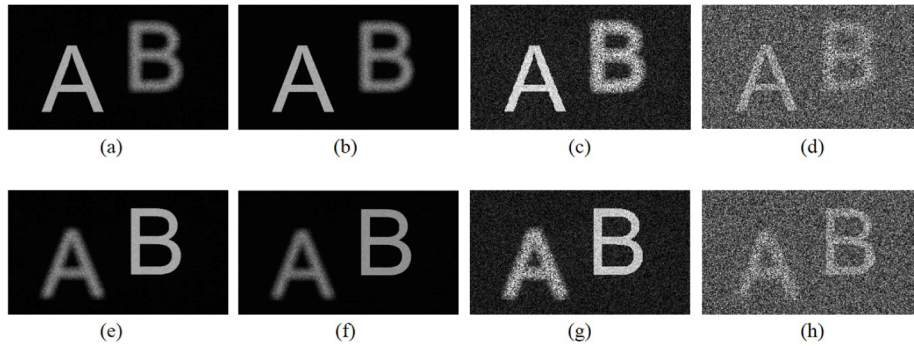


Fig. 8. Holographic 3D images numerically reconstructed using reading beams with different Gaussian distributions in phase. (a), (b), (c) and (d) are images focused on 'A'. (e), (f), (g) and (h) are images focused on 'B'. The parameters of the Gaussian distribution are  $\mu = 0 \text{ rad}$ ,  $\sigma = 0 \text{ rad}$  in (a) and (e);  $\mu = 0 \text{ rad}$ ,  $\sigma = 0.01\pi \text{ rad}$  in (b) and (f);  $\mu = 0 \text{ rad}$ ,  $\sigma = 0.05\pi \text{ rad}$  in (c) and (g);  $\mu = 0 \text{ rad}$ ,  $\sigma = 0.5\pi \text{ rad}$  in (d) and (h).

The reasons for the degradation in image quality could be the phase distortion of the output wavefront induced by the scattering of PDLC. Simulations are performed to estimate the phase distortion in the output wavefront.

The distorted phase distribution is modeled by random Gaussian distribution, which can be written as  $N(\mu, \sigma^2)$  [18], where  $\mu$  is mean of the distribution and  $\sigma$  is its standard deviation. For simplicity, the mean  $\mu$  of the Gaussian distribution is set to 0 in the simulation. And we

use Gaussian distributions with different standard deviations to describe the distortion degrees in phase. As shown in Fig. 8, we numerically reconstruct 3D images using reading beams with different Gaussian distributions in phase. As the standard deviation of phase distribution becomes larger, the image quality becomes lower. By comparing with Fig. 8, the slight degradations in Figs. 7(c) and 7(d) mean that the phase of the output wave from the backlight is close to that of an ideal plane wave. Thus, the results verify the feasibility of our proposed method.

#### 4. Conclusions

In summary, we have analyzed the DE of the design proposed in [11] based on Kogelnik's coupled-wave theory [12]. The random phase of the scattered wave is an important reason for the low DE according to the numerical results. To improve the DE, a coherent backlight using two HOEs is proposed and experimentally verified. The proposed backlight is to use a collimated elongated wave to replace the scattered wave. A laser beam spot with a size of  $\sim 0.0079 \text{ cm}^2$  is expanded to a beam with a size of  $\sim 0.7 \text{ cm}^2$  in the experiment while the slant angles of both the HOEs are  $\sim 6^\circ$ . The DE of each grating is  $\sim 21\%$  and thus the total DE of the system is  $\sim 4.3\%$ , which is one order in magnitude higher than the previous result [11]. In addition, holographic 3D images are formed with SLM using the reconstructed expanded beam. Our results suggest that the proposed backlight has a possibility to be used in the flat-panel holographic displays.

#### Appendix

Although some theoretical analyses on the hologram formed by a scattered wave and a plane wave were studied [19, 20], all these discussions used a plane wave to read the hologram. Here, an analysis on DE under the condition that the scattered wave is used as a reconstruction wave is presented. Kogelnik's coupled-wave theory [12] is used to describe the mechanism, as a phase volume hologram is formed in the experiment [11].

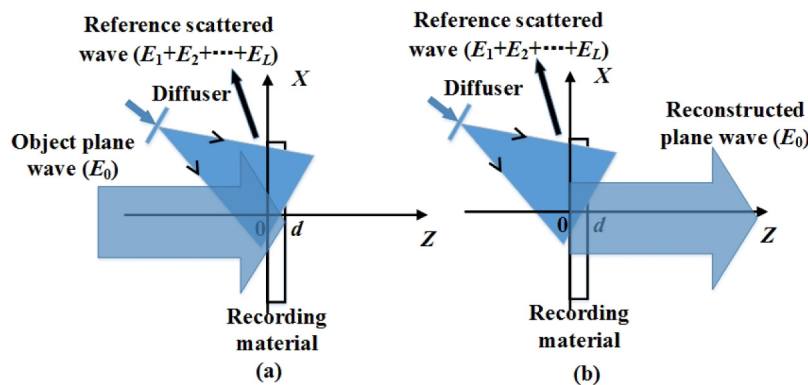


Fig. 9. Schematic diagrams of (a) recording and (b) reconstruction for the transmission volume hologram.

Suppose that the reference scattered wave consists of  $L$  plane-wave components as shown in Fig. 9. The entire field in the hologram can be written as [21]

$$E = E_0 + \sum_{l=1}^L E_l = \sum_{l=0}^L A_l \exp[-i(\mathbf{k}_l \cdot \mathbf{r} - \omega t)], \quad (3)$$

where  $E_0$  and  $\sum_{l=1}^L E_l$  represent the object plane wave and the scattered wave, respectively.  $\omega$  is the angular frequency, and  $A_l$  and  $\mathbf{k}_l$  are the complex amplitude and the wave vector of  $l$ -th plane-wave component in the sample, respectively.

During the recording process,  $L+1$  waves interfere with each other and there are  $L(L+1)/2$  gratings recorded in the hologram. In the reconstruction process, wave propagation in the hologram can be described by Helmholtz equation according to [21]

$$\nabla^2 E + k^2 \left[ n_0^2 + \sum_{g=1}^{L(L+1)/2} 2n_0 n_g \cos(\mathbf{K}_g \cdot \mathbf{r}) \right] E = 0, \quad (4)$$

where  $k = 2\pi/\lambda_0$ ,  $\lambda_0$  is the wavelength in air,  $n_0$  is the average refractive index in the sample,  $n_g$  and  $\mathbf{K}_g$  are the amplitude of refractive index modulation and wave vector of the  $g$ -th grating, respectively. According to Kogelnik's coupled-wave theory [12], the Bragg's condition can be written as

$$\mathbf{K}_g = \mathbf{k}_p - \mathbf{k}_q, \quad (5)$$

where  $\mathbf{k}_p$  and  $\mathbf{k}_q$  are the wave vectors in the sample, and the subscript  $p$  ( $q$ ) and the subscript  $g$  go over the plane-wave components and the multiple gratings, respectively.

Assume that the wave vectors of the object plane wave and the reference scattered wave are perpendicular to  $y$ -axis, and the object plane wave is normally incident onto the sample and propagates along  $z$ -axis. By substituting Eq. (3) into Eq. (4), we have

$$2ik_{lz} \frac{dA_l}{dz} = k^2 n_0 \left( \sum_{m=0}^{l-1} n_{lm} A_m + \sum_{m=l+1}^L n_{lm} A_m \right), \quad (6)$$

where  $n_{lm}$  is the amplitude of refractive index modulation of the grating that is formed by wave  $E_l$  and wave  $E_m$ ,  $k_{lz}$  is the  $z$  component of wave vector of  $l$ -th plane-wave component. Note that the complex amplitude  $A_l$  is a function of  $z$  only [12] in Eq. (6). And only the terms that satisfy Bragg's condition (Eq. (5)) are included in Eq. (6) according to [12].

The physical picture of the reconstruction process is described by Eq. (6). One can see that a plane-wave component varies in amplitude along  $z$  as coupling to the other waves. The amplitude of each wave can be calculated by solving Eq. (6) in the diffraction process.

With the assumption in the direction of propagation, the wave vector components of the object plane wave can be obtained  $k_{0x} = k_{0y} = 0$ ,  $k_{0z} = 2\pi/\lambda$ , where  $\lambda$  is the incident wavelength in the sample. To simplify the simulation, we assume that all the wave vectors of the plane-wave components in the scattered wave are perpendicular to  $y$ -axis. Therefore we have  $k_{ly} = 0$  ( $l=1 \sim L$ ) for all the plane-wave components in the scattered wave. Suppose that the angles between wave vectors of the plane-wave components in the scattered wave and axis  $z$  are from  $1^\circ$  to  $L^\circ$ , then  $k_{lz} = (2\pi/\lambda)\cos l^\circ$  ( $l=1 \sim L$ ).

The ratio of the intensity of the scattered wave to that of the object plane wave is 1:1 during the recording process, and we assume that the intensity of each plane-wave component in the scattered wave is 1. Therefore the intensities of the waves can be written as:  $|E_0|^2 = L$ ,  $|E_l|^2 = 1$  ( $l=1 \sim L$ ).

For a grating, the amplitude of refractive index modulation is proportional to the square root of the intensity product of the object wave and the reference wave ( $n_1 \propto 2\sqrt{I_O I_R}$ ) according to [21], where  $I_O$  and  $I_R$  are the intensities of object beam and reference beam, respectively. Thus one can obtain the amplitudes of refractive index modulations:

$$n_{lm} = \begin{cases} n_{10} & (l=1 \sim L, m=0) \\ n_{10}/\sqrt{L} & (l=1 \sim L, m=1 \sim L) \end{cases}, \quad (7)$$

where  $n_{lm}$  is defined in Eq. (6).  $n_0 = 1.528$ ,  $n_{10} = 0.02$  are used in the simulation according to the characteristics of polymer dispersed liquid crystal [22]. The thickness of hologram  $d$  is 50  $\mu\text{m}$ , while  $L$  is set to 10 in the simulation.

As a transmission hologram is recorded, the initial boundary conditions can be obtained as:  $A_{0(z=0)} = 0$ ,  $A_{l(z=0)} = \exp(-i\phi)$  ( $l=1\sim L$ ), where  $\phi$  is the random phase. The DE is defined as the ratio of the intensity of diffracted plane wave ( $A_{0(z=0)}A^*_{0(z=0)}$ ) to that of the reading beam ( $L$ ). The relation of DE versus distance in  $z$ -axis is shown in Fig. 1 (red triangular line).

For the comparison purposes, we assume that the plane-wave components of the scattered wave have the same initial phase, then boundary conditions can be simplified as:  $A_{0(z=0)} = 0$ ,  $A_{l(z=0)} = 1$  ( $l=1\sim L$ ). The relation between DE and distance along  $z$ -axis is plotted in Fig. 1 (black circular line).

### **Acknowledgments**

This work is supported by 973 Program (2013CB328804), National Natural Science Foundation of China (61307028, 61405114), and Science & Technology Commission of Shanghai Municipality (13ZR1420000, 14ZR1422300).